Article (Discoveries)

Small RNA activity in archaeological barley shows novel germination inhibition in response to environment

Oliver Smith[1], Sarah A. Palmer[1], Alan J. Clapham[1], Pamela Rose[2], Yuan Liu[3], Jun Wang[4], Robin G. Allaby[1*]

1 School of Life Sciences, The University of Warwick, United Kingdom.

2 The Austrian Archaeological Institute; Cairo Branch, Zamalek, Sharia Ismail Muhammed, Apt 62/72, Cairo, Egypt.

3 BGI-Europe-UK, 9 Devonshire Square, London, EC2M 4YF, UK

4 BGI-Shenzhen, Shenzhen 518083, China.

* Corresponding author (email: r.g.allaby@warwick.ac.uk)

Abstract

The recovery of ancient RNA from archaeological material could enable the direct study of micro-evolutionary processes. Small RNAs are a rich source of information because their small size is compatible with biomolecular preservation, and their roles in gene regulation make them likely foci of evolutionary change. We present here the small RNA fraction from a sample of archaeological barley generated using high-throughput sequencing that has previously been associated with localised adaptation to drought. Its microRNA profile is broadly similar to 19 globally distributed modern barley samples with the exception of three microRNAs (miRNA159, miRNA319, and miR396), all of which are known to have variable expression under stress conditions. We also found retrotransposon activity to be significantly reduced in the archaeological barley compared to the controls, where one would expect the opposite under stress conditions. We suggest that the archaeological barley's conflicting stress signals could be the result of long-term adaptation to its local environment.

Introduction

As domesticated plants were transported from their areas of origin they continued to evolve and adapt under domestication to these new environments. Such adaptations included to changes in seasonality (Yan et al. 2004; Dubcovsky et al. 2005; Fu et al. 2005; Yan et al. 2006) and to local conditions such as water stress (Araus et al. 2014). Understanding how plants became adapted to local environments is important for understanding the domestication process, and how food security issues of the past were met. Archaeological barley from the site of Qasr Ibrim, situated in the upper reaches of the Nile, is interesting because it has been identified as a crop that appears to have adapted to local water stress conditions on the basis of archaeogenetic evidence (Palmer et al. 2009; Allaby et al. 2015). The crop was grown by successive cultures from the Napatan, to the Islamic over a period of 3000 years ending a few hundred years ago.

Barley spikelet architecture generally takes one of two forms, or intermediates: two-rowed and six-rowed. Rowedness determines the number of grains per rachis node and is controlled primarily by VRS1, a transcription factor involved in suppressing lateral spikelet formation (Komatsuda et al. 2007). In many domesticated varieties, a loss-of-function mutation in the VRS1 gene (a deletion resulting in frame shift) renders the resulting *vrs1.a1* allele inactive, resulting in development of spikelets lateral to the two central spikelets and hence six rows of grain. In all cultural stages, the barley at Qasr Ibrim shows a two-row phenotype combined with the genetic basis of a six-row type. We confirmed the genetic basis of the six-rowed type in the Qasr Ibrim barley by sequencing the *vrs1* (Palmer et al. 2009) and *int-c* loci (this study, see Materials and Methods) and found both to be consistent with the respective six-rowed alleles. This suggests a reassertion of two-row over six-row

through a novel mechanism that is indicative of a strong selection pressure. The most likely pressure in this case was water stress given the aridity of the site and extremely short growing season determined by basin irrigation (Palmer et al. 2009). It is therefore interesting to establish the genomic basis of stress tolerance associated with this crop.

Archaeogenomic approaches provide a means to directly observe genomic change in the past, and have demonstrated that domesticated plants can show considerable change under domestication that could relate to local adaptation (Palmer et al. 2012). Alternatively, ancient RNA, rather than DNA, could provide a means of direct observation of phenotypes of selective value that would otherwise have been difficult to predict accurately from DNA sequence data alone. There have been few studies on ancient RNA because of concerns about its high rate of degradation (Lindahl 1996; Soukup and Breaker 1999), especially from hydrolytic attack (Thompson et al. 1995). However, under arid conditions RNA is likely to be more stable over time (Fordyce et al. 2013; Smith et al. 2014a). In particular, the small RNA fraction is of potential interest for ancient biomolecule studies of evolution because their small size (18-24 nucleotides) is about half the typical median size of ancient DNA fragments (Palmer et al. 2012), and their recovery from ancient, preserved tissues, with expected tissue specificity, has recently been demonstrated (Keller et al. 2016).

Small regulatory RNAs are a major component of gene regulation networks acting through various mechanisms including histone modifications (Gonzalez et al. 2008), DNA methylation (Li et al. 2008), translational inhibition (Baulcombe 2005) and transcription silencing (Guo et al. 2005). As such, small RNAs are critical mediators of regulatory activity in plant growth, development and

responses to biotic and environmental stresses (Talame et al. 2007; Kantar et al. 2010; Yao et al. 2010; Khraiwesh et al. 2012). The expression levels of small RNAs can vary significantly under various stresses and at different developmental stages (Bartel and Bartel 2003; Achard et al. 2004). One class of small RNA, microRNA (miRNA), are formed from conserved biogenetic pathways in which a primary microRNA transcript (pri-miRNA) forms a precursor stem loop structure (pre-miRNA) which is cleaved by a DICER-like enzyme (DCL) to produce a precise size class of miRNA molecule of 21-24 nucleotides, depending on the pathway and specific DCL involved. The miRNA is then exposed by removal of its complementary passenger strand (miRNA*) and mediated to its target through an AGO/RISC complex (Bonnet et al. 2006). MicroRNAs can be readily identified due to their highly conserved nature among flowering plants, their characteristic stem loop structures that are formed during processing (Sunkar and Zhu 2004; Axtell and Bartel 2005), and that they are often involved in highly conserved gene regulatory networks. A second class of small RNA, short interfering RNA (siRNA), are significantly less conserved between species than miRNAs and carry out a broader range of functions. The biogenetic pathway of siRNAs does not involve stem loop formation, and most mRNA have the potential to become a source of siRNAs (Carthew and Sontheimer 2009). Consequently, siRNAs are harder to predict in silico than miRNAs, but may evolve more rapidly.

To investigate the possible regulatory basis of stress tolerance in the archaeological barley from Qasr Ibrim, we isolated the small RNA fraction of the transcriptome and compared it to the small RNA fraction of 19 modern, globally distributed barley seeds. The distribution included samples from Africa, the Near East, South America, Japan, and Europe.

Results and Discussion

RNA content of archaeological seeds

On the basis of six desiccated grains dated to the Late Christian period (600-900 years BP; contextual dating), the total RNA content of the archaeological barley was determined to be three times that of the DNA content with an average of 1.45μg per seed DNA content and 4.45 μg per seed RNA content. A total of 59,702,667 reads were generated from the archaeological barley using the Illumina HiSeq 2500 platform, and an average of 696,171 reads were generated from each of the control samples using the Illumina MiSeq platform. We opted for a single-sample run using the HiSeq for the archaeological sample to pre-empt low copy numbers of microRNA as a result of diagenesis, and to compensate for possible overrepresentation of other RNA breakdown products. Of the archaeological reads generated, 59% fell into the small regulatory RNA size range, while the same average figure was 17% for the modern barley. Metagenomic analysis established that 93% of assignable reads were barley in the archaeological data set (fig. S1), which is comparable to previous analyses with cotton from the same site. To verify this, we performed a modified version of Phylogenetic Intersect Analysis pipeline (Smith et al. 2015) on a subset of reads, and found the endogenous content to be at least 87.6% (see Materials and Methods). Human contamination was found to account for only 0.01% of the assignable reads, indicating the acceptably low level of background contamination. The gross measurement of RNA and DNA content is therefore a close reflection of the true endogenous content, and indicates that RNA degradation is greatly slowed down in arid environments. A previous study calculated that at the Qasr Ibrim site ancient DNA has a half-life of 350 years (Palmer et al. 2009), and we calculated the

equivalent RNA half-like to be between 155 and 232 years. These results support a 1.5-2.3 fold higher rate of degradation of RNA than DNA if one assumes equal relative quantities of total RNA and DNA in archaeological and modern tissue, indicating that the arid preservation conditions of Qasr Ibrim decrease the relative rate at which RNA degrades compared to DNA from the 50-fold difference observed by *in vitro* studies (Eigner et al. 1961).

The composition of the barley small RNA was similar between control samples, but the archaeological sample was markedly different. The majority of reads from the archaeological sample were assigned as ribosomal at 71% compared to a mean of 23% in the control samples. tRNA and mRNA were all likewise highly overrepresented in the archaeological sample proportionally to miRNA, compared to all control samples (fig. S2). This is likely a result of RNA fragmentation during diagenesis, causing a greater proportion of breakdown products falling into the size range being studied.

Profiles of miRNAs in archaeological and control barleys

1938 HiSeq reads from a total of 59,702,667 reads were identified as known miRNAs from the archaeological barley, representing 23 families referenced against miRBase (Griffiths-Jones et al. 2008). 22053 MiSeq reads from a total of 13,227,250 representing 36 families were identified from the control samples, as expected an order of magnitude greater than the archaeological sample (table S1).

While the profiles between control samples show high levels of similarity (correlation regression matrix; all p values <0.0001), the profiles of archaeological and control samples however differ significantly; linear regression shows a low degree of correlation ($R^2 = 0.037$, $p = 0.3$). This is due to notable differences in four

miRNA families: miR159, miR319 and miR5139 both highly abundant in the archaeological sample compared to the controls, and miR396, highly abundant in the control samples compared to the archaeological sample (fig. S3). Removal of these microRNA families from statistical analysis shows that the baseline miRNA activity is similar between all samples (regression $R^2 = 0.724$, $p = < 0.0001$). The similarity of these profiles suggests that these two data sets can be directly compared meaningfully, and supports the notion that RNA frequencies can be usefully retrieved from the archaeological record.

The most notable difference between the modern and archaeological profiles was that of miR396, substantially downregulated in the archaeological barley. To detect more significant variations between the two profiles we calculated the posterior distributions of the underlying λ values giving rise to the counts observed, assuming an extended Poisson process in which the mean to variance ratio was calculated from the average of each of the pairwise counts in the two profiles (Faddy 1997), see Materials and Methods. In the cases of miR159 and miR319, we detected an up-regulation in the archaeological barley and downregulation of miR396 (fig. S4). The presence of stable expressions of three stress-related miRNAs in a range modern barleys suggests a global uniformity under unremarkable conditions, and a bimodal expression pattern in miR396 among the modern barleys further suggests two stable expression states. Conversely, the Qasr Ibrim barley significantly deviates from the modern stable expression patterns. This, coupled with phenotypic differentiation but little evidence of biomass loss, such as diminished seed size, suggests the possibility that this barley has alternate expression patterns which were an adaptation to the environment, rather than immediate stress response.

The effects of divergent miRNA profiles on barley physiology

The primary targets of the most up-regulated microRNA, miR396, are growth-regulating factor (GRF) genes (Liu et al. 2008; Debernardi et al. 2012). GRF control seed development and plant architecture and their down-regulation by miR396 in plant tissues results in growth inhibition (Rodriguez et al. 2010) and there is evidence of their association with dormancy (Martin et al. 2006). Conversely, down-regulation of miR396 itself is associated with drought stress response in rice (Zhou et al. 2010). Seemingly key to its effect is the plant's developmental stage. Extended expression during growth suppresses cell division (Rodriguez et al. 2015) whereas in mature plants, targeted blocking of it increases rice yield by allowing GRF6 expression (Gao et al. 2015). Overexpression of miR396 in rice under otherwise unstressed conditions gives rise to abnormal floret development and suggests a complex regulatory network (Liu et al. 2014). The persistent, arid paleoclimate of lower Nubia combined with the obvious difference in profiles, particularly the down-regulation of miR396 in the archaeological barley, likely suggests a stress response.

miRNAs 319 and 159 are known to share similar transcript targeting function (Li et al. 2011), and surprisingly, similar regulatory feedback mechanisms (Reichel and Millar 2015). miR319 in particular is well-known as a stress-induced regulator in agronomic plants (Zhou and Luo 2014) and miR159 is highly conserved across plants as well as being equally known for stress responses (Li et al. 2016). The primary targets of miR319 are class II TCP domain containing proteins (Schommer et al. 2008), in particular PCF5, PCF6 and GAMYB (Li et al. 2011; Thiebaut et al. 2012). To distinguish between these possibilities, we searched the messenger RNA fraction for fragments of these targets. Only trace quantities of PCF5, PCF6 and GAMYB were detected in 7 of the 19 control samples with equal representation, but in the

archaeological barley PCF transcripts were in more abundance than GAMYB transcripts by an order of magnitude. Analysis of the posterior distribution of GAMYB counts showed that the archaeological sample had fewer fragments than modern barleys, consistent with a more stringent post-transcriptional silencing in the archaeological sample (fig. S5). This result makes sense, because GAMYB is involved with the mobilization of the aleurone layer during germination, while PCF5 and PCF6 are involved in later stages of embryogenic development (Gubler et al. 1999; Kaneko et al. 2004; Thiebaut et al. 2012). GAMYB is also the target of miR159, which is the most highly expressed miRNA in the archaeological sample. In the case of the archaeological barley it seems that two miRNA loci have assumed this function in fairly equal measure. The added action of miR319 is likely to have the effect of delaying the onset of germination. In this case, the extreme difference in count is suggestive to us that the archaeological barley is responding to stress via an alternative pathway, by preventing germination via miR319 and miR159 action where miR396 is less available due to another facet of stress response. This unusual response mechanism may be due to this particular cultivar being locally adapted to the conditions at Qasr Ibrim.

GC content of archaeological RNA

Keller et al. (2016) found a small but present correlation between GC content and expression levels of mammalian microRNAs in permafrost remains using miRNA-specific qPCR, suggesting a preferential long-term survival rate for fragments with higher GC content. We compared the average GC content of identified plant miRNAs in our samples to the relative expression levels of each, and found a weak positive correlation in both ($r^2 = 0.00059$, in the ancient, and 0.00541 in the modern, fig. S6).

The fact that a stronger correlation exists in the modern samples suggests that any preferential survival of GC-rich molecules in the archaeological sample is not a significant issue. Further, the three most differentially expressed miRNAs do not deviate significantly from the median value of the GC distribution (54.2%) and the two that are highly expressed in the archaeological sample, miR159 and miR319, fall at 47.6% and 57.1% respectively. We also note that the mean GC content of miRNA in the archaeological barley (54.7%) is higher than that of the controls (53.0%), leading us to surmise that although a preferential survival of high-GC molecules is still present, the expression correlation in this case is rendered negligible by the miRNA expression profile differences between modern and archaeological samples. Other factors such as tissue type, burial conditions, and the method of data generation, which are quite different between our samples and the Tyrolean iceman, may also be at work, although a current lack of data concerning archaeological miRNAs makes further speculation difficult.

Retroelement activity in archaeological barley

To determine whether it is more likely that the miRNA expression profiles in the archaeological barley represent an immediate stress response to the environment or a more stable adaptive state, we assessed the inferred state of stress by examining evidence of retroelement activity. Increased retroelement activity under a variety of biotic and abiotic stress in plants has been well documented (Wessler 1996; Grandbastien 1998; Bui and Grandbastien 2012). A total of 57,650 reads were identified in the archaeological sample as being retroelement-targeting siRNA or retroelement transcript breakdown products. 23,313 reads in total were identified as such from the controls, with a mean frequency of 1,227 (standard deviation 348).

Adjusting for read frequency differences between multiplexed controls and expressing as a per-sample proportion, retroelement-originating reads accounted for 0.24% of all RNA species in the archaeological sample, and in the modern samples, between 0.48% and 1.78% of the total small RNA (sRNA)-sized reads with an average of 1.12% (standard deviation 0.0038). Proportions of retroelement-originating reads were therefore 4.6 times higher in the control samples but in a similar order of magnitude to the archaeological sample. We then calculated the proportions of retroelement transcripts to messenger RNA only, excluding ribosomal RNA sequences, since responsive rRNA expression is not well characterized and should not be assumed to reflect environmental stress. In this case, retroelement transcripts accounted for 0.69% of the archaeological mRNA, and between 0.67% and 2.61% in the controls, with a mean value of 1.72% (standard deviation 0.0065).

These data suggest retroelement activity in the archaeological sample is on a comparable order of magnitude to the controls, often lower, and therefore not indicative of an increased stress response relative to the controls. Previous work relating to the same sample (Smith et al. 2014b) has shown decresed retroelement expression in conjunction with increased methylation around known retroelement-containing loci. The elevated methylation patterns are likely to be a result of biotic infection noted in the sample at that stratum only, and the expectation of global genomic methylation under infections would include methylation of retroelement-containing loci, and so not be symptomatic of retroelement copy number variation. Genomic rearrangement of transposable elements in plant evolution is well documented (Palmer et al. 2012), although assessing copy number from a fragmented genome is highly error-prone. We therefore conclude that these data are congruent with our previous interpretation of normal or reduced retroelement activity.

Conclusions

The unusual two-row phenotype of the barley at Qasr Ibrim could have been formed by either a novel genetic mechanism that reasserted inhibition of the lateral florets from a six-row ancestor, or it could have been due to widespread floret failure caused by environmentally induced stress. The findings in this study of an unusual microRNA profile suggest a stress response, as do previous data of high levels of genomic methylation around retrotransposon-rich loci (Smith et al. 2014b). Our observations of normal retrotransposon activity seemingly do not support this (Table S2). However, studies of epigenetic transgenerationalism show retroelement activity in response to stress is not necessarily continuous (Ito et al. 2011). This suggests that the Qasr Ibrim barley's unique profile could be the result of localized adaptation to environmental stress, possibly over an extended period, resulting in the phenotype and genotype observed in a previous study (Palmer et al. 2009). Local adaptation is difficult to establish in the archaeological record. However, the consistency in the *vrs1* allele diverging from the expected phenotype at multiple strata observed at Qasr Ibrim, combined with all other similar studies showing an expected match between phenotype and *vrs1* allele (Mascher et al. 2016; Hagenblad et al. 2017), suggests that local adaptation is indeed present in this case.

The regulatory profiles detected in this study mostly concerned the regulation of germination and showed that distinctly different mechanisms are present between archaeological and modern barleys. The archaeological barley was significantly more inhibited by miRNA319 and miR159 that would likely have the cause of preventing germination in a mechanism unique to this cultivar. In the case of the modern counterparts, miR396 appears to take this role; in fact, stress-induced down-regulation

of miR396 in the archaeological barley could have resulted in the alternative mechanism seen in the archaeological barley, which over several generations has become stabilized as an adaptation. This regulatory difference makes sense given the basin irrigation system in which the archaeological barley was grown. In ancient Nubia the length of the growing season (*Peret*) was determined by the Nile flood and the ensuing time it took for the soil to dry out again, about 120 days (Kemp 2006). The length of this season corresponds very closely to the length of time required for barley to grow. Consequently mechanisms that prevent early onset of germination, before the floods, may well have been important to avoid a high mortality of seedlings.

This study is the second to recover ancient small regulatory RNA and shows that it can be meaningfully used to contrast how ancient organisms fared in their environment relative to their modern counterparts. We suggest that the evidence presented here shows that the archaeological barley was adapted through stress responses to the agrarian environment around the Nile as exemplified through its differential regulation of germination and floral structure. Such examples of local adaptation highlight the increasingly probable notion that epigenetic regulation is a driver for evolution, and the possibility that some issues of food security in the past may have been better addressed than in the present.

Materials and Methods.

Samples

Archaeological barley from Qasr Ibrim from the Late Christian horizon (1100-1400 AD) was supplied by Dr Clapham. 15 accessions of modern barley were supplied by the USDA: PI 642783 (Giza), PI 182613 (Japan), PI 392528 (South Africa), PI

510559 (Peru), PI 524707 (Egypt), PI290743 (Kenya), PI 100121 (India), PI 65216 (China), PI 524708 (Egypt dryland), PI 168904 (Argentina), PI 490393 (Mali), PI 642787 (Giza), CIho5059 (Australia), GSHO842 (Japan). 2 accessions were supplied by the John Innes Centre: B9604 (Iraq) and B7297 (Iran). 2 accessions were supplied by NIAB: Tipple and Line 14 hulled (both U.K.).

Nucleic acid extraction

All ancient nucleic acids were handled in a dedicated ancient DNA laboratory. RNA was isolated using a modified protocol of the Ambion MirVana RNA isolation kit. 6 grains from the same archaeological context were extracted in bulk as a single sample. Modifications included an extended incubation time in 2% CTAB buffer (5 days at 37˚C) followed by a single chloroform extraction and isopropanol precipitation, before resuspending the RNA pellet in the supplied binding buffer and continuing the protocol as per the manufacturer's instructions. Because the vast majority of archaeological RNA fragments already exist within the target size for column based enrichment of small fragments (<300 nt), this step was deemed unnecessary and omitted to avoid further loss of molecules. RNA was extracted from control samples in a separate, non-PCR laboratory using a modified protocol of the Ambion MirVana RNA isolation kit. Crushed seeds were incubated for 1 hour at 65˚C in 2% CTAB buffer followed by a single chloroform extraction and ispropanol precipitation. Due to the high starch content of modern grains compared to the archaeological, RNA pellets were dissolved in SSTE buffer to remove polysaccharides, and RNA re-precipitated with isopropanol. Pellets were resuspended in the supplied binding buffer and the protocol was completed according to manufacturer's instructions. Small RNA fragments (<300 nt) were enriched using the manufacturer's column-based method. Since mechanical size enrichment of this type

has not been reported to introduce sequence bias, we do not anticipate this modification influenced the results. Further, we do not see any order-of-magnitude differences in reported relative expression from similarly-sized transcripts such as transposable elements or ribosomal transcripts, suggesting the differences in protocol introduce minimal, if any, bias into our molecular classification. RNA for all samples were quantified using the Qubit RNA assays.

Illumina library construction and sequencing

A singleplex library was created for the archaeological sample using an Air Small RNA Library Preparation Kit (Bioo Scientific, cat. no 5130, discontinued) according to manufacturer's instructions, and run as a single lane on the Illumina HiSeq platform by BGI (Shenzen, China). Control sample libraries were made using a NextFlex Small RNA Sequncing Kit (Bioo Scientific, cat. no. 5132-06) due to multiplexing allowances, again following the manufacturer's protocol. We used standard indexing primers for multiplexing, and run on the Illumina MiSeq platform using a v2 reagent kit. All library enrichment took place using 8 PCR cycles, and all sequencing runs took place with 50 rounds of sequencing.

Bioinformatic methods

Primary data processing (format conversion, removal of adapter sequences, parsing into 18-25 sRNA-sized sequences and identification of sequence frequencies in reads) was carried out using scripts of the author's design. The majority of pattern matching exercises were performed using bowtie version 0.12. Separate bowtie indexes were created for each molecule type from corresponding fasta files: complete barley genome cultivar Morex, mature plant miRNA from mirbase, complete graminae retroelements from Michigan State University's Plant Repeat Database, and individual genes of interest (PCF5, PCF6 and GaMyb) from NCBI. In all cases of

bowtie pattern matching, a single mismatch was allowed in the archaeological sample but only where a positive-strand C>U or negative strand G>A base modification occurred. This was to compensate for postmortem deamination known to occur in ancient nucleic acids (Gilbert et al. 2005). For the control samples, exact matches only were considered positive.

No comprehensive list of primary miRNA transcripts exists, so a database was created based on homologous pre-miRNA stem loop sequences. Pri-miRNA sequence data for all available plant species was downloaded from mirbase and subjected to BLAST searching against a database created from the barley cultivar Morex genome (contigs of ~100-800 nt each). Pre-miRNA sequences matching to the Morex genome under standalone BLASTn parameters were considered to be homologous if originated in other plant species. Morex contigs to which homologous stem-loop sequences matched were considered to be representative of miRNA primary transcripts. These contigs were extracted and converted to a bowtie index to which the Illumina sequences of archaeological and control samples were matched, again allowing a single deamination mismatch in the archaeological sample.

For metagenomic analysis, sequences were processed using standalone blastn, using the complete nucleotide (nt) database and pre-set parameters for short sequences ('blastn-short'), which reduces word size values to 7 over the default 11. This was deemed the most appropriate method due to the ultrashort nature of sequences being evaluated.

Phylogenetic Intersect Analysis (PIA) was performed on a subset of reads to verify the expected levels of endogenous miRNAs, by proxy of confidence in their taxonomic assignations. Plant small RNA fractions are typically ultrashort and highly conserved, and this poses challenges for discriminant phylogenetic analyses such as

PIA. Essentially, many sRNA sequences are so highly conserved, and by virtue of their sizes are often coincidentally present in non-plants, they are unresolvable from almost a basal level on the phylogenetic tree. To account for this, we took 10,000 redundant sequences and ran them through the PIA pipeline as normal. We disregarded those sequences whose second BLAST hit had an identical score to the first, then filtered the remaining reads by disregarding those with an unknowable classification intersect value. We then re-mapped the remaining reads to the barley genome. Finally, we assessed the number of exogenous reads by isolating those meeting two criteria: not mapping to the genome, and not consistent with a putative barley assignation under PIA (i.e. not being assigned at any taxonomic node leading to barley). We then applied redundancy frequencies to these data to calculate the overall proportions of endogenous and exogenous reads. We found the endogenous content of the barley to be at least 87.6%, and the accuracy of PIA to be 80.6%, both values being consistent with our previous estimates (Palmer et al. 2012; Smith et al. 2015).

Int-c alleles of Qasr Ibrim barley

Barley architecture is controlled by both *VRS1* and *INT-C* genes (Ramsay et al. 2011). To check whether the two-row phenotype of the Qasr Ibrim barley could be accounted for by a combination of *vrs1* and *int-c* alleles which have been known to be responsible for a two-row phentotype (Ramsay et al. 2011) despite the presence of the 6-row associated *vrs1.a1* allele. We mapped 6,731 Illumina genomic DNA reads generated from seeds of the same archaeological deposit as the miRNA-associated sample to all five alleles of the *int-c* locus, using bowtie2. A single *int-c* genotype

(*Int-c.a*; Genbank accession KY070602) was found in the Qasr Ibrim barley across samples, which is the *vrs1* allele associated with the 6 row phenotype.

GC content estimation

GC content for sequences matching conserved miRNAs (Table S1) was calculated and sequences were sorted into incremental bins of GC%, at 0.1% increments. Since multiple forms of each miRNA exist and were identified, the GC content for any given miRNA species within and between samples is not constant. Therefore, sequence identities of the three differentially expressed miRNAs miR159, miR319 and miR396 were then identified, and the bins containing the majority of those sequences for each sample were designated as the 'GC location' for the relevant miRNA, Figure S6 and Table S3.

Half-life estimation

To estimate the half-life of RNA at the site, we used a per-seed calculation from modern and archaeological barleys since per-mass calculations would be skewed due to desiccation. We observed a mean RNA value of 4.45 μg per seed in the archaeological, and 65.2 μg per seed in the modern sample of the closest geographical match (Giza). We then calculated the RNA half-life ($T_{1/2}$) using the equation:

$$T_{1/2} = (T \times \log 2) / (\log (V_1 / V_2))$$

Where T is the elapsed time, V_1 is the amount of modern RNA in μg, and V_2 is the amount of archaeological RNA in μg. We used archaeological dates of the Late Christian sample of 900-600 years BP to calculate the half-life estimation of 155-232 years.

Statistical methods

Comparability of miRNA frequencies between control samples was confirmed using a correlation regression matrix in GraphPad Prism (version 6.1 for Mac, GraphPad Software, La Jolla California USA). Frequencies of conserved miRNA families were normalized between the control samples by dividing the frequency of each miRNA family in each sample by the ratio of total miRNA frequency to total reads in that sample, and then multiplying that value by the mean ratio of total miRNA frequencies to total reads (0.00165). The adjusted values were then used to normalize the miRNA frequencies of the archaeological sample, by calculating the mean adjusted total miRNA frequency per control (1145.5) and dividing this by the total miRNA frequency of the archaeological sample to give an adjustment ratio of 0.59. Raw frequencies of miRNA families in the archaeological sample were multiplied by this ratio to give an adjusted frequency. Comparisons of modern and archaeological were simplified for graphical representation by calculating the normalized mean of all control samples for each miRNA family and plotting these values against normalized archaeological reads for each miRNA family. Standard deviations between controls were expressed as error bars (fig. 1).

Likelihood kernels were generated using a standard Poisson process for Figures 4 and 5 where low copy numbers occurred (<50). Large RNA count numbers are known to deviate from pure Poisson processes (Hebenstreit et al. 2011), but extended Poisson processes are robust for describing counts (Faddy 1997). In the case of miRNA populations we estimated the ratio of variance to mean by taking point estimates of mean, variance and ratio (r) of normalized miRNA counts for each miRNA, and obtained the average value. The likelihood kernel was then based on a Normal approximation of an extended Poisson process using a variance equal to the product of the mean and the ratio (r), using equation 5.1a.a of (Leonard and Hsu

2001). The likelihoods show the relative likelihood for the underlying mean count number giving rise to the observed counts in each case. In the case of GaMyb, PCF5 and PCF6 fragments, we corrected frequencies within the controls by taking the arithmetic mean of matching fragments across all samples and then calculating the mean ratio from the relative endogenous ratios across all controls. This was done to compensate for low-frequency fragments being over- or under-represented considering an average individual correction factor of 279 between modern and ancient, this factor stemming from the level of data generated (controls were 19-plexed on MiSeq versus, 1-plex HiSeq 2000 for the archaeological).

Acknowledgements

This work was supported by the Biotechnology and Biological Research Council (grant number BBSRC DTA BBG0177941). The authors would like thank the Egyptian Exploration Society for access to the material from Qasr Ibrim.

References

Achard P, Herr A, Baulcombe DC, Harberd NP. 2004. Modulation of floral development by a gibberellin-regulated microRNA. Development 131: 3357-3365.

Allaby RG, Gutaker R, Clarke A, Pearson N, Ware R, Palmer S, Kitchen JL, Smith O. 2015. Using archaeogenomics and computational approaches to unravel the history of local adaptation in crops. Philos Trans R Soc Lond, Ser B: Biol Sci 370.

Araus JL, Ferrio JP, Voltas J, Aguilera M, Buxó R. 2014. Agronomic conditions and crop evolution in ancient Near East agriculture. Nat Commun 5: 3953.

Axtell MJ, Bartel DP. 2005. Antiquity of microRNAs and their targets in land plants. Plant Cell 17: 1658-1673.

Bartel B and Bartel DP. 2003. MicroRNAs: at the root of plant development? Plant Physiol 132: 709-717.

Baulcombe D. 2005. RNA silencing. Trends Biochem Sci 30: 290 - 293.

Bonnet E, Van de Peer Y, Rouze P. 2006. The small RNA world of plants. New Phytol 171: 451 - 468.
Bui Q, Grandbastien M-Al 2012. LTR Retrotransposons as Controlling Elements of Genome Response to Stress? In Grandbastien M.-A. l., Casacuberta J. M., editors. Plant Transposable Elements Volume **24**, Berlin, Heidelberg: Springer. p 273-296.
Carthew RW, Sontheimer EJ. 2009. Origins and mechanisms of miRNAs and siRNAs. Cell 136: 642-655.
Debernardi JM, Rodriguez RE, Mecchia MA, Palatnik JF. 2012. Functional specialization of the plant miR396 regulatory network through distinct microRNA-target interactions. PLoS Genet 8: e1002419.
Dubcovsky J, Chen C, Yan L. 2005. Molecular characterization of the allelic variation at the VRN-H2 vernalization locus in barley. Mol Breed 15: 395-407.
Eigner J, Boedtker H, Michaels G. 1961. The thermal degradation of nucleic acids. Biochim Biophys Acta 51: 165-168.
Faddy MJ. 1997. Extended Poisson Process Modelling and Analysis of Count Data. Biometrical J 39: 431-440.
Fordyce SL, Avila-Arcos MC, Rasmussen M, Cappellini E, Romero-Navarro JA, Wales N, Alquezar-Planas DE, Penfield S, Brown TA, Vielle-Calzada J-P, et al. 2013. Deep Sequencing of RNA from Ancient Maize Kernels. PLoS One 8: e50961.
Fu D, Szucs P, Yan L, Helguera M, Skinner JS, von Zitzewitz J, Hayes PM, Dubcovsky J. 2005. Large deletions within the first intron in VRN-1 are associated with spring growth habit in barley and wheat. Mol Genet Genomics 273: 54-65.
Gao F, Wang K, Liu Y, Chen Y, Chen P, Shi Z, Luo J, Jiang D, Fan F, Zhu Y. 2015. Blocking miR396 increases rice yield by shaping inflorescence architecture. Nat Plants 2: 15196.
Gilbert MT, Bandelt HJ, Hofreiter M, Barnes I. 2005. Assessing ancient DNA studies. Trends Ecol Evol 20: 541-544.
Gonzalez S, Pisano DG, Serrano M. 2008. Mechanistic principles of chromatin remodeling guided by siRNAs and miRNAs. Cell Cycle 7: 2601-2608.
Grandbastien M-Al. 1998. Activation of plant retrotransposons under stress conditions. Trends Plant Sci 3: 181-187.
Griffiths-Jones S, Saini H, van Dongen S, Enright A. 2008. miRBase: tools for microRNA genomics. Nucleic Acids Res 36: D154 - 158.

Gubler F, Raventos D, Keys M, Watts R, Mundy J, Jacobsen JV. 1999. Target genes and regulatory domains of the GAMYB transcriptional activator in cereal aleurone. Plant J 17: 1-9.
Guo H-S, Xie Q, Fei J-F, Chua N-H. 2005. MicroRNA directs mRNA cleavage of the transcription factor NAC1 to downregulate auxin signals for arabidopsis lateral root development. The Plant Cell Online 17: 1376-1386.
Hagenblad J, Morales J, Leino MW, Rodríguez-Rodríguez AC. 2017. Farmer fidelity in the Canary Islands revealed by ancient DNA from prehistoric seeds. J Archaeol Sci 78: 78-87.
Hebenstreit D, Fang M, Gu M, Charoensawan V, van Oudenaarden A, Teichmann SA. 2011. RNA sequencing reveals two major classes of gene expression levels in metazoan cells. Mol Syst Biol 7: 497.
Ito H, Gaubert H, Bucher E, Mirouze M, Vaillant I, Paszkowski J. 2011. An siRNA pathway prevents transgenerational retrotransposition in plants subjected to stress. Nature 472: 115-119.
Kaneko M, Inukai Y, Ueguchi-Tanaka M, Itoh H, Izawa T, Kobayashi Y, Hattori T, Miyao A, Hirochika H, Ashikari M, et al. 2004. Loss-of-function mutations of the rice GAMYB gene impair alpha-amylase expression in aleurone and flower development. Plant Cell 16: 33-44.
Kantar M, Unver T, Budak H. 2010. Regulation of barley miRNAs upon dehydration stress correlated with target gene expression. Functional & Integrative Genomics 10: 493-507.
Keller A, Kreis S, Leidinger P, Maixner F, Ludwig N, Backes C, Galata V, Guerriero G, Fehlmann T, Franke A, et al. 2016. miRNAs in ancient tissue specimens of the Tyrolean Iceman. Mol Biol Evol. 34 (4): 793-801
Kemp B. 2006. Ancient Egypt: Anatomy of a civilization. Oxford: Routledge Press.
Khraiwesh B, Zhu J-K, Zhu J. 2012. Role of miRNAs and siRNAs in biotic and abiotic stress responses of plants. Biochim Biophys Acta 1819: 137-148.
Komatsuda T, Pourkheirandish M, He CF, Azhaguvel P, Kanamori H, Perovic D, Stein N, Graner A, Wicker T, Tagiri A, et al. 2007. Six-rowed barley originated from a mutation in a homeodomain-leucine zipper I-class homeobox gene. Proc Natl Acad Sci U S A 104: 1424-1429.
Leonard T, Hsu JSJ. 2001. Bayesian Methods. Cambridge: Cambridge University Press.

Li XY, Wang XF, He K, Ma YQ, Su N, He H, Stolc V, Tongprasit W, Jin WW, Jiang JM, et al. 2008. High-resolution mapping of epigenetic modifications of the rice genome uncovers interplay between DNA methylation, histone methylation, and gene expression. Plant Cell 20: 259-276.
Li Y, Alonso-Peral M, Wong G, Wang M-B, Millar AA. 2016. Ubiquitous miR159 repression of MYB33/65 in Arabidopsis rosettes is robust and is not perturbed by a wide range of stresses. BMC Plant Biol 16: 179.
Li Y, Li C, Ding G, Jin Y. 2011. Evolution of MIR159/319 microRNA genes and their post-transcriptional regulatory link to siRNA pathways. BMC Evol Biol 11: 122.
Lindahl T. 1996. Endogenous damage to DNA. Philos Trans R Soc Lond B Biol Sci 351: 1529-1538.
Liu H, Guo S, Xu Y, Li C, Zhang Z, Zhang D, Xu S, Zhang C, Chong K. 2014. OsmiR396d-Regulated OsGRFs Function in Floral Organogenesis in Rice through Binding to Their Targets OsJMJ706 and OsCR4. Plant Physiol 165: 160-174.
Liu H-H, Tian X, Li Y-J, Wu C-A, Zheng C-C. 2008. Microarray-based analysis of stress-regulated microRNAs in Arabidopsis thaliana. RNA 14: 836-843.
Martin RC, Liu P-P, Nonogaki H. 2006. microRNAs in seeds: modified detection techniques and potential applications. Can J Botany 84: 189-198.
Mascher M, Schuenemann VJ, Davidovich U, Marom N, Himmelbach A, Hubner S, Korol A, David M, Reiter E, Riehl S, et al. 2016. Genomic analysis of 6,000-year-old cultivated grain illuminates the domestication history of barley. Nat Genet 48: 1089-1093.
Palmer SA, Clapham AJ, Rose P, Freitas FbO, Owen BD, Beresford-Jones D, Moore JD, Kitchen JL, Allaby RG. 2012. Archaeogenomic evidence of punctuated genome evolution in gossypium. Mol Biol Evol 29: 2031-2038.
Palmer SA, Moore JD, Clapham AJ, Rose P, Allaby RG. 2009. Archaeogenetic evidence of ancient Nubian barley evolution from six to two-row indicates local adaptation. PLoS One 4: e6301 (Electronic version).
Ramsay L, Comadran J, Druka A, Marshall DF, Thomas WTB, Macaulay M, MacKenzie K, Simpson C, Fuller J, Bonar N, et al. 2011. INTERMEDIUM-C, a modifier of lateral spikelet fertility in barley, is an ortholog of the maize domestication gene TEOSINTE BRANCHED 1. Nat Genet 43: 169-172.
Reichel M, Millar AA. 2015. Specificity of plant microRNA target MIMICs: Cross-targeting of miR159 and miR319. J Plant Physiol 180: 45-48.

Rodriguez RE, Ercoli MF, Debernardi JM, Breakfield NW, Mecchia MA, Sabatini M, Cools T, De Veylder L, Benfey PN, Palatnik JF. 2015. MicroRNA miR396 Regulates the Switch between Stem Cells and Transit-Amplifying Cells in Arabidopsis Roots. The Plant Cell 27: 3354-3366.
Rodriguez RE, Mecchia MA, Debernardi JM, Schommer C, Weigel D, Palatnik JF. 2010. Control of cell proliferation in Arabidopsis thaliana by microRNA miR396. Development 137: 103-112.
Schommer C, Palatnik JF, Aggarwal P, Chételat A, Cubas P, Farmer EE, Nath U, Weigel D. 2008. Control of jasmonate biosynthesis and senescence by miR319 targets. PLoS Biol 6: e230.
Smith O, Clapham A, Rose P, Liu Y, Wang J, Allaby RG. 2014a. A complete ancient RNA genome: identification, reconstruction and evolutionary history of archaeological Barley Stripe Mosaic Virus. Sci Rep 4: 4003.
Smith O, Clapham AJ, Rose P, Liu Y, Wang J, Allaby RG. 2014b. Genomic methylation patterns in archaeological barley show de-methylation as a time-dependent diagenetic process. Sci Rep 4:5559.
Smith O, Momber G, Bates R, Garwood P, Fitch S, Pallen M, Gaffney V, Allaby RG. 2015. Sedimentary DNA from a submerged site reveals wheat in the British Isles 8000 years ago. Science 347: 998-1001.
Soukup GA, Breaker RR. 1999. Relationship between internucleotide linkage geometry and the stability of RNA. RNA 5: 1308-1325.
Sunkar R, Zhu JK. 2004. Novel and stress-regulated microRNAs and other small RNAs from Arabidopsis. Plant Cell 16: 2001-2019.
Talame V, Ozturk NZ, Bohnert HJ, Tuberosa R. 2007. Barley transcript profiles under dehydration shock and drought stress treatments: a comparative analysis. J Exp Bot 58: 229-240.
Thiebaut F, Rojas CA, Almeida KL, Grativol C, Domiciano GC, Lamb CRC, De Almeida Engler J, Hemerly AS, Ferreira PCG. 2012. Regulation of miR319 during cold stress in sugarcane. Plant Cell Environ 35: 502-512.
Thompson JE, Kutateladze TG, Schuster MC, Venegas FD, Messmore JM, Raines RT. 1995. Limits to Catalysis by Ribonuclease A. Bioorg Chem 23: 471-481.
Wessler SR. 1996. Plant retrotransposons: Turned on by stress. Curr Biol 6: 959-961.

Yan L, Fu D, Li C, Blechl A, Tranquilli G, Bonafede M, Sanchez A, Valarik M, Yasuda S, Dubcovsky J. 2006. The wheat and barley vernalization gene VRN3 is an orthologue of FT. Proc Natl Acad Sci U S A 103: 19581-19586.

Yan L, Helguera M, Kato K, Fukuyama S, Sherman J, Dubcovsky J. 2004. Allelic variation at the VRN-1 promoter region in polyploid wheat. Theor Appl Genet 109: 1677-1686.

Yao Y, Ni Z, Peng H, Sun F, Xin M, Sunkar R, Zhu J-K, Sun Q. 2010. Non-coding small RNAs responsive to abiotic stress in wheat (*Triticum aestivum L.*). Funct Integr Genomics 10: 187-190.

Zhou L, Liu Y, Liu Z, Kong D, Duan M, Luo L. 2010. Genome-wide identification and analysis of drought-responsive microRNAs in Oryza sativa. J Exp Bot 61: 4157-4168.

Zhou M, Luo H. 2014. Role of microRNA319 in creeping bentgrass salinity and drought stress response. Plant Signaling & Behavior 9: e28700.

Figures and tables

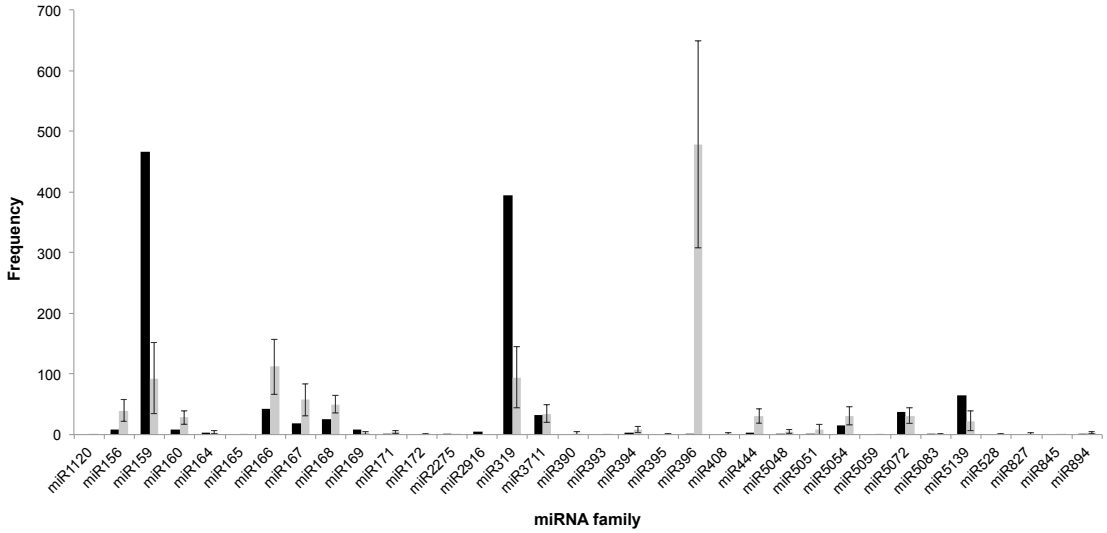

Figure 1: Comparison of conserved miRNA levels in archaeological and modern barleys. Frequencies of the modern barleys have been normalized and collated into a single bar for display purposes. The black series represents the archaeological sample and the grey series represents the controls. Error bars represent standard deviation between control samples.

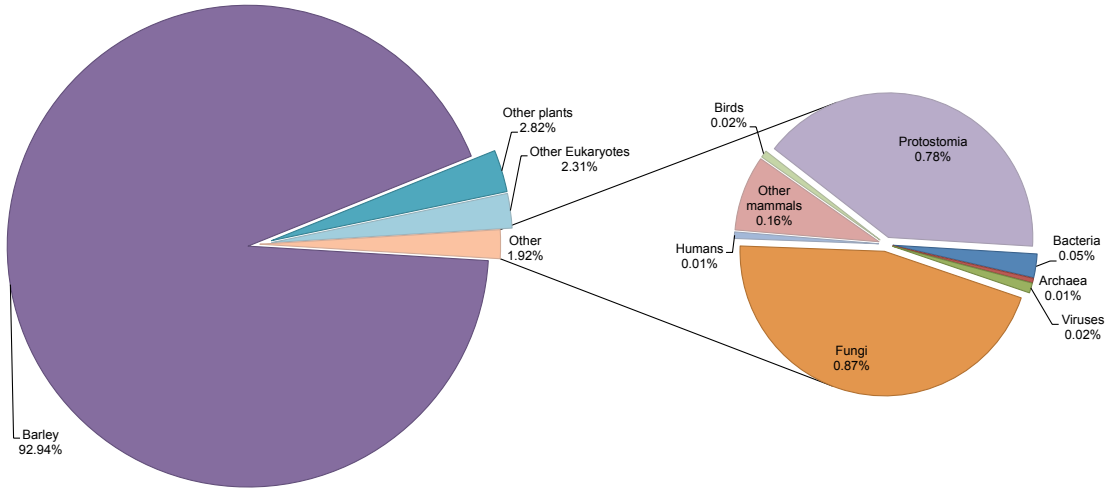

Figure S1: Metagenomic breakdown of Illumina reads from the archaeological barley. The unusually low level of contamination in this sample suggests the authenticity of the Illumina data generated from it.

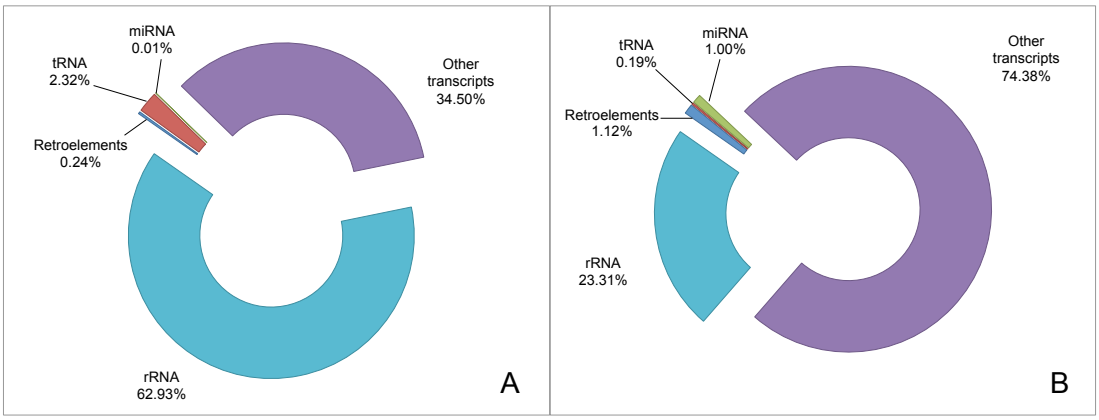

Figure S2: Breakdown of RNA classes. Panel A: Archaeological, actual values. Panel B: modern samples, mean values.

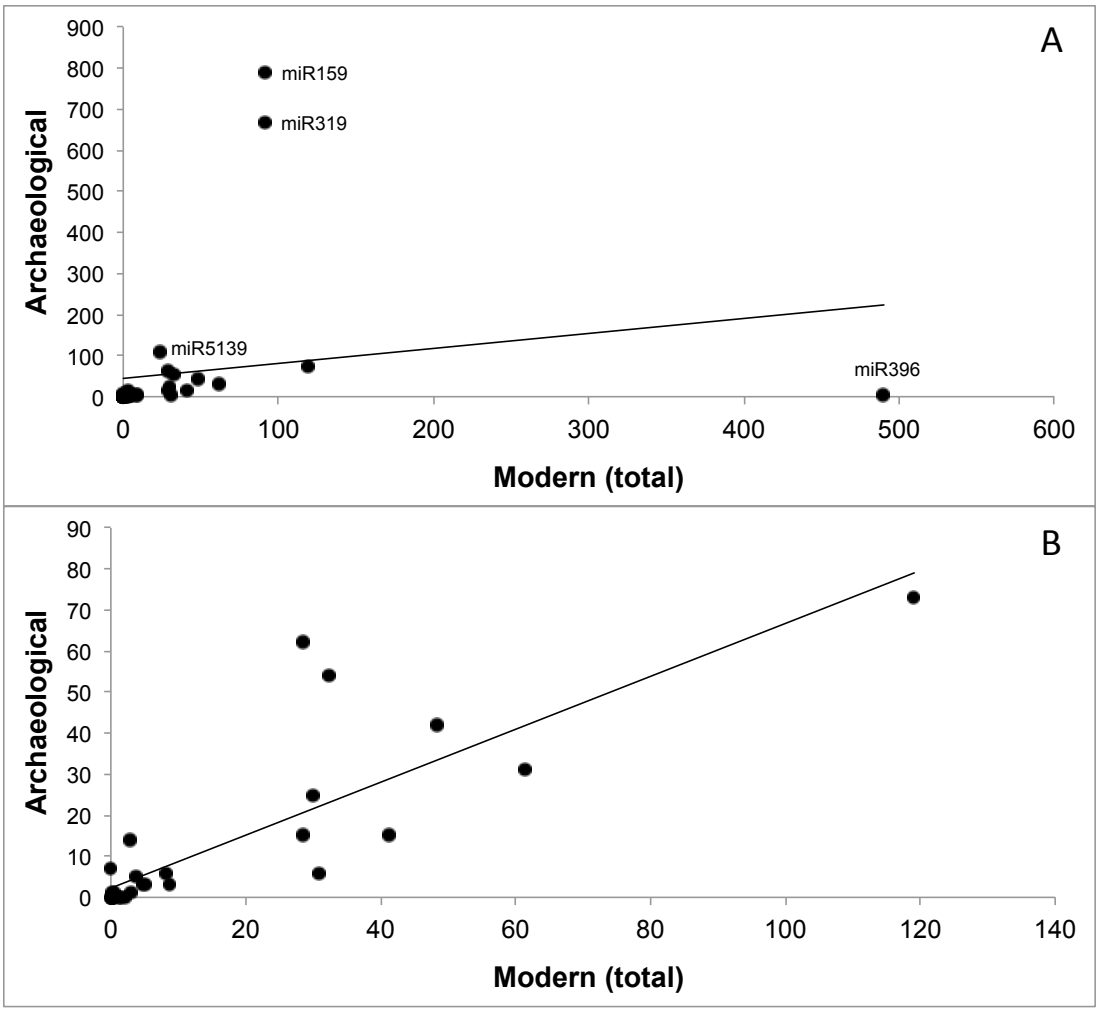

Figure S3: Linear regressions of modern and archaeological barleys. Panel A, including miR159, miR319 and miR396. Panel B; increased correlation of background miRNA species following removal of major functional species.

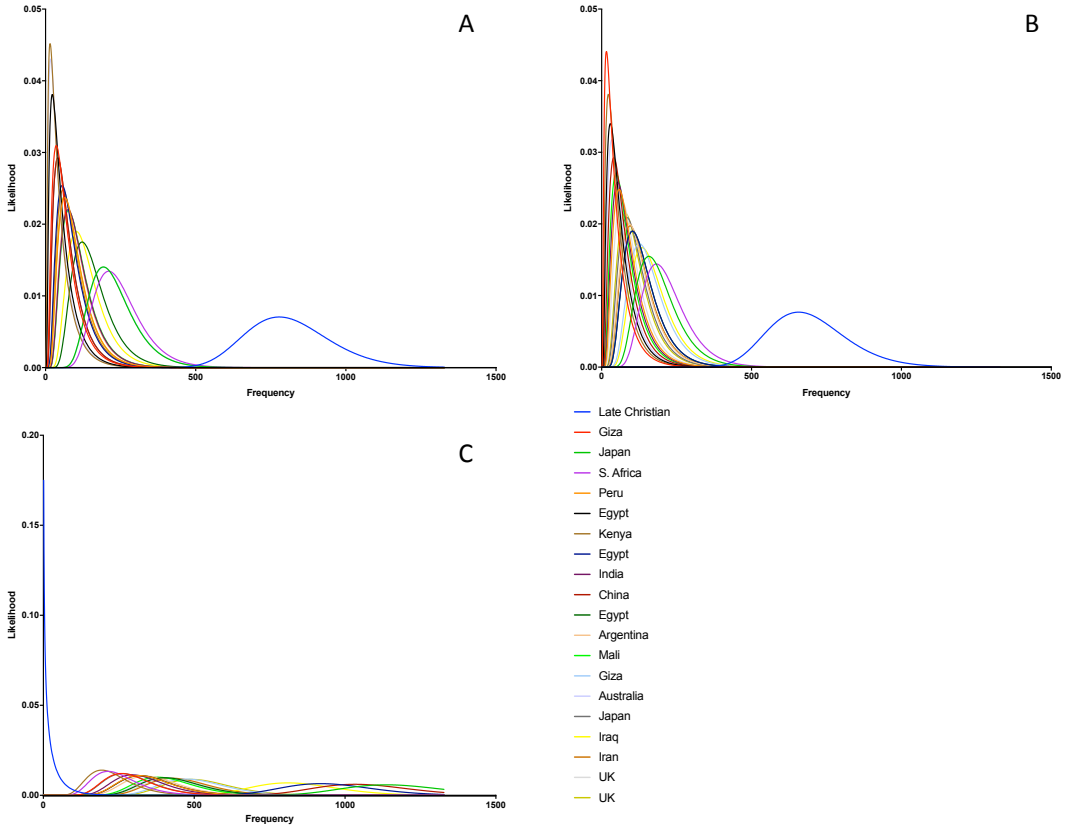

Figure S4: Posterior Poisson distributions of three differentially expressed microRNAs across archaeological (blue) and modern (others) barleys. Panel A: miR159. Panel B: miR319. Panel C: miR396.

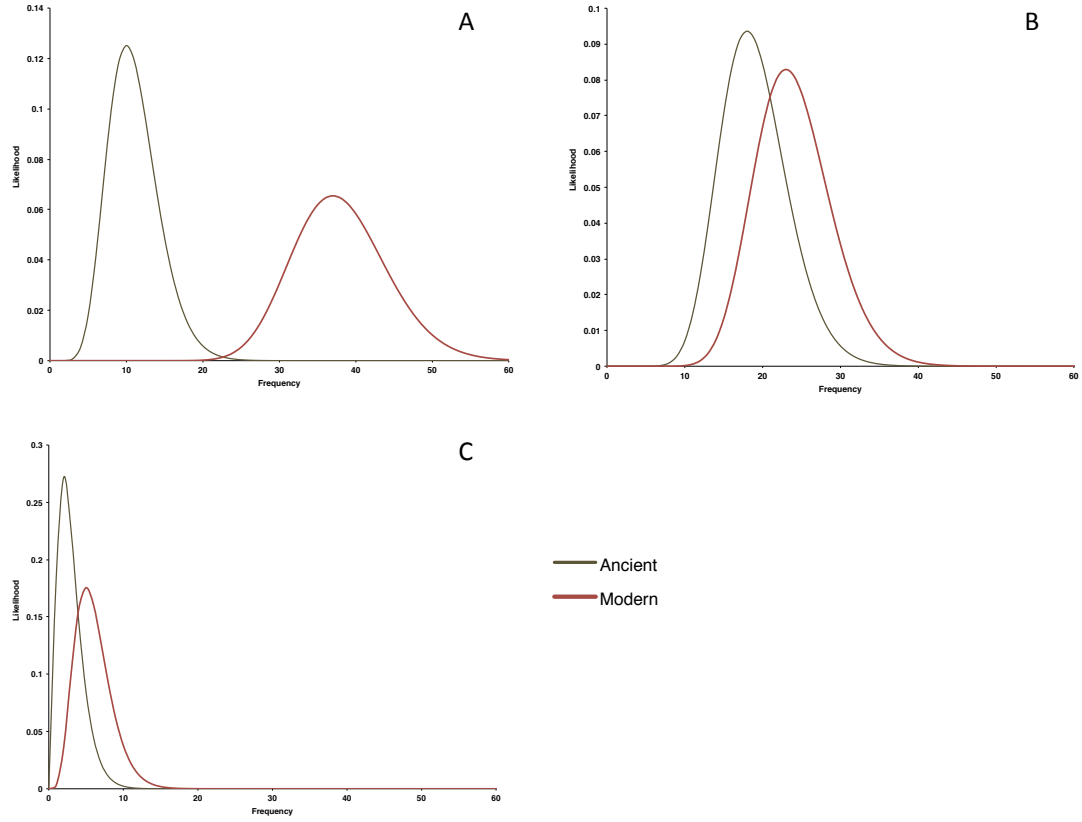

Figure S5: Posterior Poisson distribution of class II TCP domain-containing proteins targeted by miR396. Panel A: GAMYB. Panel B: PCF5. Panel C: PCF6.

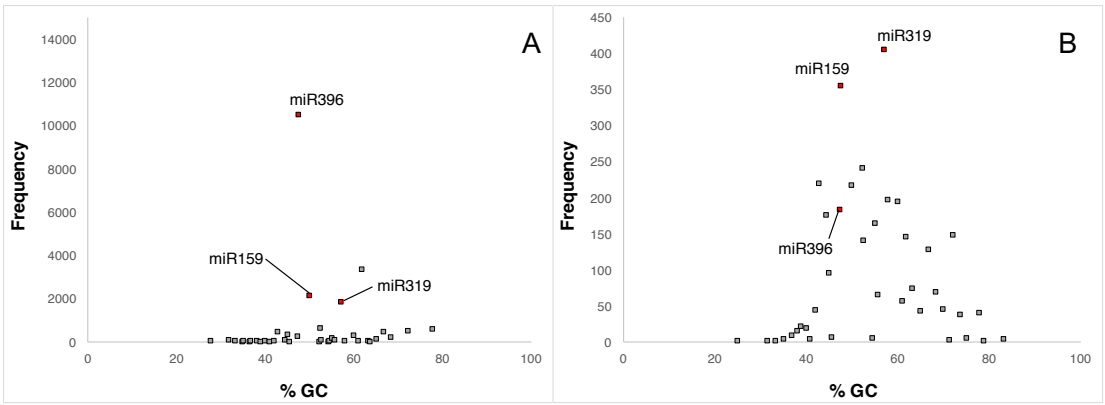

Figure S6: Frequency of miRNA reads according to GC content. GC content for all conserved microRNA reads was calculated and placed into bins of 0.1%. The three most differentially expressed miRNA species (miR159, miR319 and miR396) are highlighted as red data points, placed where the average GC content of the reads identified as such falls into that bin. We note a weak positive correlation between frequency and GC content for all samples. Panel A: summed modern values. Panel B: archaeological values.

	Archaeological	Modern control samples																		
miRNA Family	1	1	2	3	4	5	6	7	8	9	10	11	12	13	14	15	16	17	18	19
	Late Chrisitan	Giza	Japan	S. Africa	Peru	Egypt	Kenya	Egypt	India	China	Egypt	Argentina	Mali	Giza	Australia	Japan	Iraq	Iran	UK	UK
miR1120	0	0	2	0	0	0	0	0	0	0	0	0	0	1	0	0	0	0	0	0
miR156	15	2	144	36	28	13	23	35	42	57	29	38	67	57	38	29	56	21	37	31
miR159	790	48	204	222	75	32	24	66	86	51	133	84	87	205	26	51	114	69	88	74
miR160	15	8	55	1	29	23	21	16	48	39	44	22	29	36	18	24	30	29	21	50
miR164	5	0	10	1	3	3	5	2	5	8	11	4	3	3	2	1	2	1	6	3
miR165	0	0	0	0	0	1	0	0	0	0	0	0	0	1	0	0	0	0	0	0
miR166	73	22	445	133	75	66	40	100	151	144	133	118	142	183	63	77	100	81	77	113
miR167	31	12	264	34	35	40	50	64	56	69	47	61	82	86	34	58	67	45	26	36
miR168	42	29	64	38	43	38	25	23	60	68	60	41	52	96	35	48	52	41	46	60
miR169	14	1	2	0	3	1	1	2	0	4	10	5	1	8	5	1	2	3	3	3
miR171	3	1	4	1	5	5	6	1	9	4	9	3	11	8	3	4	1	4	4	4
miR172	0	0	0	0	1	0	1	0	0	1	1	0	0	0	0	0	0	0	1	0
miR2275	1	0	1	0	0	0	0	0	0	0	0	0	0	0	0	1	0	0	0	0
miR2916	7	0	0	0	0	0	0	0	0	0	0	0	0	0	0	0	0	0	0	0
miR319	669	25	169	194	69	39	32	114	64	51	114	103	59	137	44	95	146	106	77	90
miR3711	54	22	22	4	41	38	36	36	28	32	39	38	35	31	24	12	52	53	29	44
miR390	0	0	4	1	0	3	5	1	5	0	3	1	2	8	0	1	2	2	2	1
miR393	0	0	0	0	0	1	0	0	1	0	0	0	0	0	0	0	0	1	0	0
miR394	6	2	19	0	8	8	7	8	8	7	15	6	6	16	0	11	6	6	11	13
miR395	0	0	0	0	0	1	0	0	0	1	1	1	1	0	0	0	0	0	3	0
miR396	3	271	1149	226	330	332	205	931	307	1045	415	350	391	485	407	274	822	441	431	502
miR408	0	2	0	0	0	1	2	1	4	4	1	3	1	1	1	0	1	3	2	0
miR444	6	14	61	5	30	26	18	28	19	33	53	31	40	63	16	16	31	30	28	47
miR5048	3	4	25	2	5	3	5	4	1	4	5	6	2	8	5	5	4	4	3	3
miR5051	3	4	71	12	5	2	4	18	1	3	4	3	5	3	2	12	4	1	6	6
miR5054	25	14	28	4	55	40	36	44	23	34	35	35	33	34	28	12	38	34	7	35
miR5059	0	0	0	0	0	0	0	0	0	0	1	0	1	0	0	0	0	0	0	0
miR5072	62	37	11	23	38	19	34	20	33	45	34	37	27	46	26	21	33	17	15	28
miR5083	1	0	0	0	0	0	0	0	0	2	1	0	0	0	2	0	0	1	0	0
miR5139	109	13	61	37	19	9	10	15	24	112	18	23	13	33	32	15	6	5	7	6
miR528	0	2	0	0	0	0	0	2	0	0	0	0	1	0	0	0	0	0	0	0
miR827	0	2	0	0	0	3	4	2	1	2	1	1	2	2	0	0	0	3	4	0
miR845	0	0	0	0	0	0	0	0	0	0	1	0	0	0	0	0	0	0	0	0
miR894	1	3	3	2	4	0	1	7	2	0	1	3	4	7	3	0	4	2	2	8
Total	1938	536	2818	976	901	747	595	1540	978	1820	1219	1017	1097	1558	814	768	1573	1003	936	1157
Total reads for each	Not applicable	541759	941447	741158	696256	490405	454368	756179	538418	644253	640912	684441	579008	790111	764536	656373	996102	675880	893175	742469
Ratio miRNA of total	Not applicable	0.00098937	0.002993265	0.001316858	0.001294064	0.001523231	0.001309511	0.002036555	0.001816433	0.002824977	0.001901977	0.001485884	0.00189462	0.001971875	0.001064698	0.001170066	0.001579156	0.001483991	0.001047947	0.001558314

Table S1: Raw read counts of conserved miRNA in modern and archaeological barleys. Ratios of miRNA to total read number are shown as basis for correction between miRNA families in the modern samples. The corrected values are then used to calculate a second correction factor to compare all modern samples against the archaeological sample (adjusted data not shown).

		Archaeological	Modern control samples																	
	Sample	1	1	2	3	4	5	6	7	8	9	10	11	12	13	14	15	16	17	18	19
		Late Chrisitan	Giza	Japan	S. Africa	Peru	Egypt	Kenya	Egypt	India	China	Egypt	Argentina	Mali	Giza	Australia	Japan	Iraq	Iran	UK	UK
	Total (18-25 size)	24011053	39833	195508	133217	110352	71135	64618	151656	77360	107584	190533	138556	105123	158101	145498	109559	157275	113248	132951	135439
miRNA	mRNA (total)	8302629	25165	139866	95505	70634	45782	39034	113210	47777	72444	65973	96286	66865	108701	110573	84108	108965	67054	70232	74764
	Retroelements	57650	529	1706	642	1671	1197	1147	1801	1246	1451	1389	1258	1362	1382	879	768	1389	1141	953	1404
	Other mRNA	8244979	24636	138160	94863	68963	44585	37887	111409	46531	70993	64584	95030	65503	107319	109694	83340	107576	65913	69279	73360
	Proportion retroelements	0.69%	2.10%	1.22%	0.67%	2.37%	2.61%	2.94%	1.59%	2.61%	2.00%	2.11%	1.30%	2.04%	1.27%	0.79%	0.91%	1.27%	1.70%	1.36%	1.88%
	rRNA	15110652	9287	46381	36665	23619	14866	12234	38030	15311	24759	22163	35787	22028	40570	47197	35940	41023	21944	22701	22601

Table S2: Raw counts of reads assigned as specific RNA types in archaeological and modern barleys.

Modern		Archaeological	
% GC	Freqency	% GC	Freqency
27.8	6	25.0	1
31.8	73	31.6	1
33.3	9	33.3	1
34.8	2	35.0	3
35.0	14	36.8	8
36.4	4	38.1	14
36.8	7	38.9	21
38.1	40	40.0	18
38.9	2	40.9	3
40.0	17	42.1	43
40.9	3	42.9	219
42.1	6	44.4	175
42.9	424	45.0	95
44.4	47	45.5	6
45.0	319	47.4	183
45.5	3	47.6	354
47.4	238	50.0	216
47.6	10470	52.4	241
50.0	2134	52.6	140
52.2	1	54.5	4
52.4	598	55.0	164
52.6	70	55.6	65
54.2	1	57.1	405
54.5	6	57.9	197
55.0	158	60.0	194
55.6	49	61.1	56
57.1	1834	61.9	145
57.9	33	63.2	73
60.0	287	65.0	42
61.1	39	66.7	128
61.9	3335	68.4	68
63.2	37	70.0	45
63.6	2	71.4	2
65.0	105	72.2	148
66.7	444	73.7	37
68.4	191	75.0	4
72.2	505	77.8	40
77.8	569	78.9	1
		83.3	3

Table S3: GC content of identified miRNA, after figure S6. Sequences were ordered into bins of GC content at 0.1% increments. Red shading indicates GC bin of the majority of miR396-associated reads, blue indicates miR159-associated reads, and green indicates miR319-associated reads. GC bins are calculated based on miRNA matches within the sample; since multiple forms of each miRNA exist, the exact GC content of a single designation (e.g. miR159) varies between samples. For example, while only 3 miR396 sequences were identified in the archaeological sample, their mean GC content clusters with others, hence their clustering with 180 other sequences.